

Introduction

Immiscible fluid-fluid displacement in porous media is ubiquitous in many practical applications. It is well known that the transport phenomenon is strongly affected by both capillary number Ca and viscosity (i.e., mobility) ratio M , while the combined effects of them in topologically disordered porous media are less understood. In this study, we investigate the fluid displacement of drainage under varied disorder conditions for different combinations of Ca and M using the pore network model (PNM). Firstly, we propose a modified Delaunay tessellation method for pore-network extraction of 3D disordered porous media. By comparing with simulation results from the lattice Boltzmann method as benchmark for both simple- and multi-phase flow, it is shown that the proposed method more accurately captures the pore structure and compares favourably against two other popular pore-network extraction approaches. Then, the dynamic PNM is adopted to study immiscible fluid displacement processes across a wide range of flow conditions and fluid properties in porous media of different disorder, covering the flow regimes including capillary fingering, viscous fingering and stable displacement.

Under favourable displacement conditions, i.e., $M > 1$, an increase in disorder promotes unstable fingering invasion as opposed to stable displacement. Under unfavourable condition with $M < 1$, the transition from capillary towards viscous fingering regime occurs at lower Ca for porous media with more disordered pore structures.

This study extends the classical phase diagram of immiscible displacement by taking the topological disorder into account, highlighting the impact of microstructure disorder on fluid transport processes in porous media.

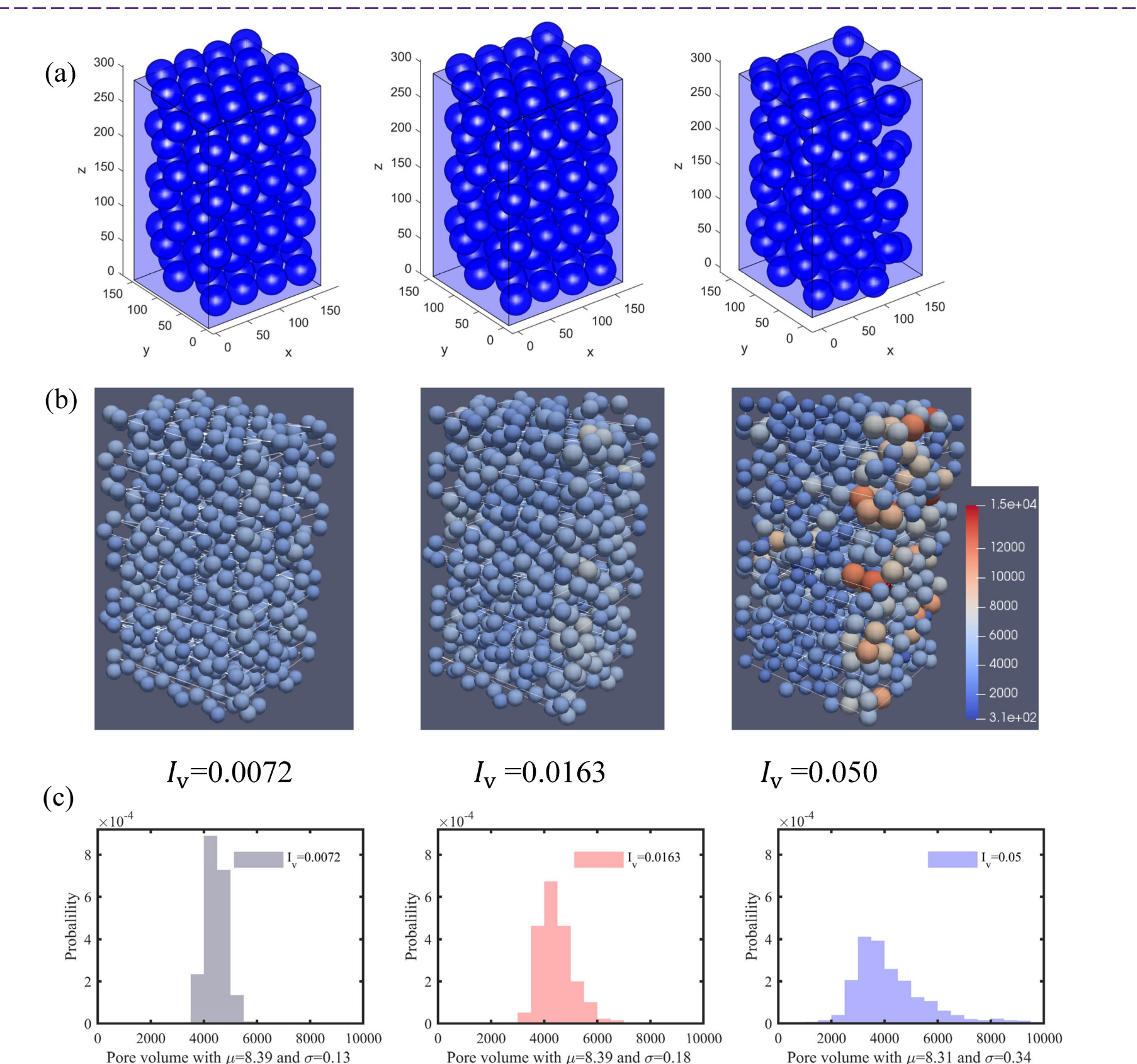


Figure 1: (a) Generated disordered media for LBM simulations and (b) their corresponding pore network for PNM simulations. The colour legend refers to the pore volume. (c) Pore volume distributions under Delaunay tessellation.

Method

Disorder packing

The disordered granular media is generated based on iterative Monte-Carlo movement of each sphere obstacle. The disorder index is analyzed via the Voronoi tessellation as

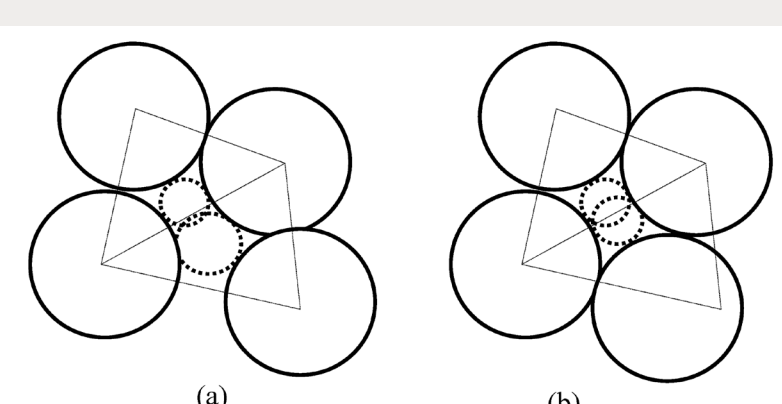
$$I_v = \{ \langle \phi_i^2 \rangle - \langle \phi_i \rangle^2 \}^{1/2}$$

where the operator $\langle \cdot \rangle$ denotes to volume average, and ϕ_i denotes the porosity of each Voronoi cell.

Pore network modelling

Two modified Delaunay tessellation is employed to partition the pore space of disordered packing based on merging of adjacent Delaunay cells, named MDT-L and MDT-S, see below (a) and (b), respectively¹.

An open-source package, OpenPNM is used to simulate the single-phase flow in the generated pore-networks. Two phase-drainage flow is studied using numSCAI, an open-source simulator for dynamic pore-network modelling.



Lattice Boltzmann modelling

The Shan-Chen multi-component lattice Boltzmann modelling is adopted to verify the above pore-network modelling approaches. The Shan-Chen multi-component LBM

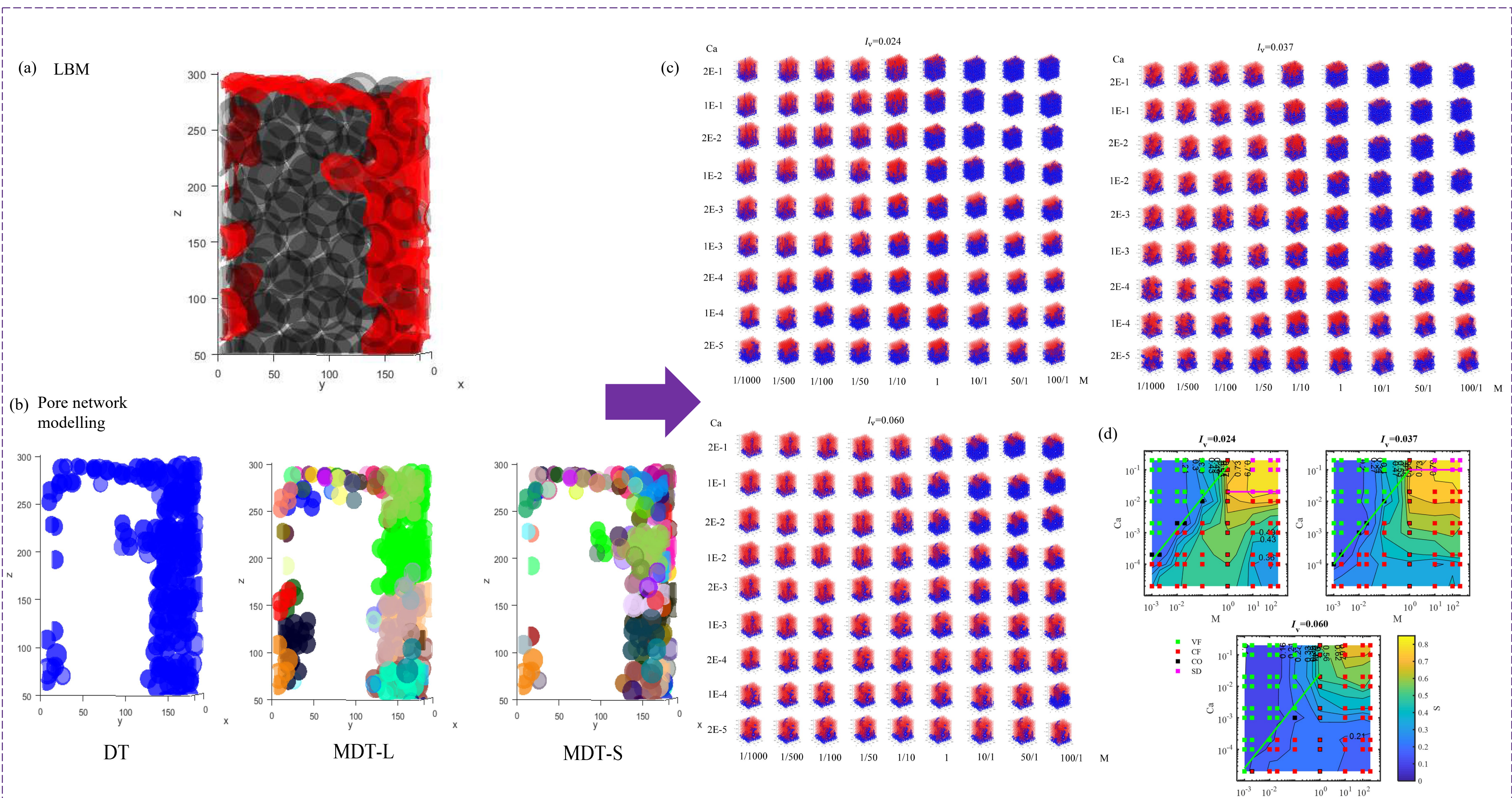


Figure 2: (a) The fluid distribution at the breakthrough point from LBM. The red colour represents the invading fluid and grey represents the sphere obstacles. (b) The fluid distribution from the pore network invasion percolation under varied merging criteria including the DT, MDT-L and MDT-S. In the MDT-L and MDT-S, different arbitrary colours represent different merged pores. After the verification of PNM, (c) shows flow patterns for different disordered media under varied capillary number and mobility ratio. The red and blue denote the oil and water occupied pores, respectively. (d) The Ca - M phase diagram for disordered packing, referred to the fluid displacement pattern in (c). The green and pink lines represent the VF-CF and CF-SD phase boundary lines, respectively.

Results

Comparison of PNM and LBM in two phase flow

Delaunay tessellation (DT) and its two modified versions based on merging adjacent tetrahedrons (MDT-S and MDT-L) are presented for characterizing pore space in porous media, which is an essential process in the PNM. Firstly, the performance of three different tessellation methods is made by the comparison with two-phase LBM results. Secondly, the selected tessellation method is adopted to study the dynamic behavior of drainage patterns for varied disordered media at different Ca and M .

Three disordered porous media with $I_v = 0.0072, 0.0163, 0.05$, seen in Fig. 1(a), are generated using 128 spheres. Fig. 1(b) demonstrates the corresponding pore networks of disordered packing, constructed based on the Delaunay tessellation (DT). Fig. 1(c) illustrates the pore volume distribution with different I_v . In addition to DT, two modified tessellation methods are introduced based on merging adjacent tetrahedrons (i.e., MDT-S and MDT-L). A large Delaunay cell is high likely to merge with its adjacent ones in MDT-L, resulting in a large pore volume along with deleting large throats in the common faces, compared with the DT and MDT-S. Among different tessellation methods including the DT, MDT-S and MDT-L, the most accurate one needs to be confirmed via the following numerical benchmarks.

The comparison of two-phase flow is shown in Fig. 2(a) and (b) to verify varied pore tessellation methods and algorithms for quasi-static drainage in the PNM. We select the previous generated porous medium with $I_v = 0.05$ as an input geometry. In LBM, the fluid-fluid displacement is simulated under the two-component Shan-Chen model. In the PNM, the pore network for the packing with $I_v = 0.05$ is firstly built using the DT, MDT-S and MDT-L. Then the invasion percolation is adopted in OpenPNM to model the fluid-fluid displacement in the quasi-static drainage.

The statistical comparison between the PNM and the LBM is made from both the macroscopic level and pore by pore basis, including the invading efficiency S^* and the comparison of each individual pore so that the performance of varied pore space tessellation methods can be precisely measured.

Table 1 below summarises the statistic comparison in the quasi-static drainage between the LBM and PNM under varied merging criteria, and the macroscopic relative errors are all within 5%. It can be concluded that the pore network from all three merging criteria can successfully predict the invading efficiency. However, the MDT-S shows a better consistency with the LBM during the pore-scale comparison with the smallest pore-scale relative error and the highest Pearson correlation that is the closest to 1.

	DT	MDT-L	MDT-S	LBM
S^*	0.3221	0.3162	0.3061	0.3116
RE_m	3.37%	1.79%	-1.76%	-
RE_p	9.36%	12.7%	8.42%	-
ρ_x	0.78	0.74	0.81	-

Acknowledgements

We are grateful for the technical inputs by Dr Zhongzheng Wang, Yixiang Gan from the University of Sydney.

References

- 1 Al-Raoush, R., Thompson, K., & Willson, C. S. (2003). Comparison of Network Generation Techniques for Unconsolidated Porous Media. *Soil Science Society of America Journal*, 67(6), 1687. <https://doi.org/10.2136/sssaj2003.1687>

Dynamic drainage

With previous verified MDT-S, the pore network model proves to be an efficient way for drainage modelling. Three Large-scale disordered media consisting of 768 spheres with $I_v = 0.024, 0.037, 0.060$ are generated and used for studying drainage patterns at different Ca and M .

The displacement patterns at the breakthrough point under different capillary number Ca and mobility ratio M are plotted in Fig. 2(c), which illustrate the significant impact of Ca and M on the displacement patterns. Due to the competition of viscous and capillary forces, at a high Ca , the viscous fingering patterns are observed when $M < 1$, while $M > 1$ represents the stable displacement patterns. The capillary fingering occurs with a low Ca , regardless of M . The contour plots of saturation at the breakthrough point for $I_v = 0.024, 0.037, 0.060$ are made in Fig. 2(d). For $M < 1$, it is found that the increase of Ca reduces the breakthrough saturation, whereas an increase in Ca boosts the invading efficiency for $M > 1$. The simulated tendency shows the consistency with other experimental and numerical studies. Regarding the disorder effect, as shown in Fig. 2(c), a higher I_v corresponds to more chance to develop a viscous fingering at a given Ca and M when $M < 1$, while the high degree of disorder indicates a less stable displacement for $M > 1$.

Conclusions

In this study, a comprehensive comparison of drainage flow in porous media has been made between the pore network model and the lattice Boltzmann simulation.

- The comparison illustrates that the modified Delaunay tessellation with slightly merging adjacent Delaunay cells is suitable for generating the pore-network on a sphere-based porous medium. This provides an alternative for successfully constructing the pore-network.
- The pore-to-pore validation between the LBM and PNM further demonstrates the competence of current proposed PNM. This work shows that the PNM can be a first choice for simulating the fluid path in granular media due to its extreme low computation cost.
- Using the verified tessellation method, the two-phase dynamic drainage patterns in disordered porous media are modelled at varying capillary number and mobility ratio, with mapping full Ca - M phase diagrams including the capillary and viscous fingering and stable displacement.
- The disorder can impact the phase boundary line, through shifting downward the VF-CF phase boundary line and shifting upward the CF-SD phase boundary line. Consequently, the disorder promotes the viscous fingering phenomenon and hinders the stable displacement, which is unfavorable for an efficiency fluid-fluid displacement, especially in the field of oil recovery.

To overcome the fingering phenomenon, the wise selection of injected fluid and velocity is of importance and the developed phase diagrams provides a basis for the controlled fluid patterns under varied capillary number and mobility ratio for the studied porous medium.